Predictions of light hadronic decays of heavy quarkonium $^1D_2$ states in nonrelativistic QCD

Ying Fan,* Zhi-Guo He,† Yan-Qing Ma,‡ and Kuang-Ta Chao§

Department of Physics and State Key Laboratory of Nuclear Physics and Technology, Peking University, Beijing 100871, China

(Received 26 March 2009; published 6 July 2009)

The inclusive light hadronic decays of $^1D_2$ heavy quarkonia are studied within the framework of the nonrelativistic QCD at the leading order in v and up to the order of α_s^3. With one-loop QCD corrections, the infrared divergences and Coulomb singularities in the decay amplitudes are proved to be absorbed by the renormalization of the matrix elements of corresponding nonrelativistic QCD operators, and the infrared finite short-distance coefficients are obtained through the matching calculations. By taking the factorization scale to be $2m_Q$, the light hadronic decay widths are estimated to be about 274, 4.7, and 8.8 KeV for η_{c2}, η_{b2}, and η'_{b2}, respectively. Based on the above estimates, and using the E1 transition width and dipion transition width for η_{c2} estimated elsewhere, we get the total width of η_{c2} to be about 660–810 KeV, and the branching ratio of the E1 transition $\eta_{c2} \to \gamma h_c$ to be about (44–54)%, which will be useful in searching for this missing charmonium state through, e.g., $\eta_{c2} \to \gamma h_c$ followed by $h_c \to \gamma \eta_c$.

DOI: 10.1103/PhysRevD.80.014001 PACS numbers: 12.38.Bx, 12.39.St, 13.20.Gd

I. INTRODUCTION

The studies of production and decay mechanisms for heavy quarkonia provide important information on both perturbative and nonperturbative QCD. Based on the nonrelativistic (NR) nature of heavy quarkonium systems, an effective field theory, the nonrelativistic QCD (NRQCD) factorization formalism was proposed by Bodwin, Braaten, and Lepage in the 1990s [1]. Within this framework, the inclusive decay and production of heavy quarkonium can be factorized into two parts, the short-distance coefficients and the long-distance matrix elements. Differing from the color-singlet model (CSM) [2], in the NRQCD factorization formalism, the heavy quark and antiquark pair annihilated or produced at short distances can be in both the color-singlet and the color-octet states with the same or different angular momentum quantum numbers [1], and the latter is known as the color-octet mechanism. This mechanism has been used to remove the infrared divergences in inclusive P-wave charmonium production [3] and decay [1,4–6] to give the infrared safe and model independent predictions.

Recently, the inclusive light hadronic decays of ^3D_J charmonium states were also studied within the framework of NRQCD factorization up to order α_s^3 [7,8]. The infrared divergence found in the CSM calculation [9] is removed by absorbing it into the matrix elements of the color-octet ^3P_J operators. Furthermore, the new contributions at order α_s^2 from the color-octet ^3P_J and $^3S_1$ matrix elements enhance the decay widths of ^3D_J states, and the numerical results are larger than those estimated in the CSM by several times in magnitude [8]. One can expect that a similar case will emerge in the inclusive light hadronic decay of $^1D_2$ charmonium, namely, the η_{c2} state. The difference between the η_{c2} and ^3D_J states is that there are no infrared divergences in the inclusive decay width of η_{c2} in the CSM up to order α_s^2 [10], and the numerical result is about 110 KeV [11]. However, the infrared divergence will emerge again in the decay width of η_{c2} in the CSM at order α_s^3, which needs to be removed by invoking the color-octet mechanism, i.e. by absorbing it into the corresponding color-octet matrix elements.

On the other hand, the estimation of the inclusive light hadronic decay width of η_{c2} is also important phenomenologically for probing this missing charmonium state. Quark model predicts its mass within the range 3.80–3.84 GeV [12,13], which lies between the $D\bar{D}$ and the $D^*\bar{D}$ thresholds. However, its odd parity ($J^{PC} = 2^{-+}$) forbids the decay to $D\bar{D}$. As a result, it should be a narrow state, and its main decay modes are the electric as well as hadronic transitions to lower-lying charmonium states and the inclusive light hadronic decay. Therefore, the study for the inclusive light hadronic decay of η_{c2} in NRQCD factorization will provide important information on searching for this state in high-energy $p\bar{p}$ collision [14], in B decays [15], in higher charmonium transitions, and in the low-energy $p\bar{p}$ reaction in PANDA at FAIR [16] and in the e^+e^- process in BESIII at BEPC [17].

In this paper, we study the one-loop QCD corrections to light hadronic decay of $^1D_2$ within the framework of NRQCD factorization. The paper is organized as follows: after an introduction of the NRQCD factorization formalism in Sec. II, we calculate the decay widths up to $\mathcal{O}(\alpha_s^3)$ in perturbative QCD in Sec. III, where both the real and virtual corrections are considered. Then perturbative NRQCD is applied to obtain the imaginary parts of the forward scattering amplitudes in Sec. IV. Combined with the QCD results, the infrared divergences are either canceled or absorbed into the long-distance NRQCD matrix elements, and the finite short-distance coefficients are ob-

*ying.physics.fan@gmail.com
†hzgzlh@gmail.com
‡yqma.cn@gmail.com
§ktchao@th.phy.pku.edu.cn

tained. Together with the long-distance matrix elements estimated by solving the operator evolution equations, the decay width is determined. The numerical results and phenomenological discussions are given in Sec. V. Finally, we will give a brief summary of our results in Sec. VI.

II. GENERAL FORMULAS

There are four important scales in the heavy quarkonium system: the heavy quark mass m_Q, the typical momentum of the heavy quark or the inverse of the size of the bound state $m_Q v$,[1] the binding energy $m_Q v^2$, and the QCD scale $\Lambda_{\rm QCD}$, while the dynamical property of the bound state is mainly determined by the latter three scales. Thus, one can choose a cutoff μ_Λ with condition $m_Q > \mu_\Lambda \gg m_Q v (m_Q v^2, \Lambda_{\rm QCD})$ to integrate out the hard scale m_Q. Expanding the nonlocal effective action in power of v and writing the result in the two-component Pauli spinor space, one then can get the effective Lagrangian for NRQCD [1]

$$\mathcal{L}_{\rm NRQCD} = \mathcal{L}_{\rm light} + \mathcal{L}_{\rm heavy} + \delta\mathcal{L}, \tag{1}$$

where the Lagrangian $\mathcal{L}_{\rm light}$ describes gluon and light quarks. At leading order in v, the heavy quark and antiquark are described by $\mathcal{L}_{\rm heavy}$

$$\mathcal{L}_{\rm heavy} = \psi^\dagger\left(iD_t + \frac{\mathbf{D}^2}{2m_Q}\right)\psi + \chi^\dagger\left(iD_t - \frac{\mathbf{D}^2}{2m_Q}\right)\chi, \tag{2}$$

where ψ denotes the Pauli spinor field that annihilates a heavy quark, χ denotes the Pauli spinor field that creates a heavy antiquark, and D_t and $\mathbf{D}$ are the time and space components of the gauge-covariant derivative D^μ, respectively. The relativistic corrections to $\mathcal{L}_{\rm heavy}$ are included in the term $\delta\mathcal{L}$. The most important correction terms for heavy quarkonium energy splitting are the bilinear ones:

$$\begin{aligned}\delta\mathcal{L}_{\rm bilinear} = {} & \frac{c_1}{8m_Q^3}[\psi^\dagger(\mathbf{D}^2)^2\psi - \chi^\dagger(\mathbf{D}^2)^2\chi] \\ & + \frac{c_2}{8m_Q^2}[\psi^\dagger(\mathbf{D}\cdot g\mathbf{E} - g\mathbf{E}\cdot\mathbf{D})\psi \\ & + \chi^\dagger(\mathbf{D}\cdot g\mathbf{E} - g\mathbf{E}\cdot\mathbf{D})\chi] \\ & + \frac{c_3}{8m_Q^2}[\psi^\dagger(i\mathbf{D}\times g\mathbf{E} - g\mathbf{E}\times i\mathbf{D})\cdot\boldsymbol{\sigma}\psi \\ & + \chi^\dagger(i\mathbf{D}\times g\mathbf{E} - g\mathbf{E}\times i\mathbf{D})\cdot\boldsymbol{\sigma}\chi] \\ & + \frac{c_4}{2m_Q}[\psi^\dagger(g\mathbf{B}\cdot\sigma)\psi - \chi^\dagger(g\mathbf{B}\cdot\boldsymbol{\sigma})\chi],\end{aligned} \tag{3}$$

where $E^i = G^{0i}$ and $B^i = \frac{1}{2}\epsilon^{ijk}G^{jk}$ are the electric and magnetic components of the gluon field-strength tensor $G^{\mu\nu}$, respectively.

In the Lagrangian $\mathcal{L}_{\rm NRQCD}$ in (1), there are still three low-energy scales: the soft scale $m_Q v$, the ultrasoft scale $m_Q v^2$, and the QCD scale $\Lambda_{\rm QCD}$. The existence of multiscales makes the power counting rules of NRQCD (the velocity scaling rules [1]) generally nonhomogeneous. More seriously, if one wants to do the NRQCD loop calculations in a dimensional regularization scheme with $\mathcal{L}_{\rm NRQCD}$ defined in (1), one will find that the hard scale cannot decouple from the loop integrals and the power counting rules are inevitably violated [18]. These problems can be solved simultaneously by the method of regions [19], which will be explained and applied in our calculations in Sec. IV.

To reproduce the annihilation contribution to a low-energy $Q\bar{Q} \to Q\bar{Q}$ scattering amplitude in NRQCD, local four-fermion operators in $\delta\mathcal{L}$ are needed, which have the general form [1]

$$\delta\mathcal{L}_{\text{4-fermion}} = \sum_n \frac{f_n(\mu_\Lambda)}{m_Q^{d_n-4}}\mathcal{O}_n(\mu_\Lambda), \tag{4}$$

where $\mathcal{O}_n$ denotes regularized local four-fermion operators, such as $\psi^\dagger\chi\chi^\dagger\psi$, and d_n is the naive scaling dimension of the operator. The dependence on cutoff μ_Λ of the operator $\mathcal{O}_n$ is canceled by that of scaleless coefficient $f_n(\mu_\Lambda)$, which can be computed by matching the full QCD onto the NRQCD as perturbation series in α_s.

In NR theory, the width of heavy quarkonium H is -2 times the imaginary part of the energy of the state, thus one has [1]

$$\begin{aligned}\Gamma(H \to LH) &= 2\,\mathrm{Im}\langle H|\delta\mathcal{L}_{\text{4-fermion}}|H\rangle \\ &= \sum_n \frac{2\,\mathrm{Im} f_n(\mu_\Lambda)}{m_Q^{d_n-4}}\langle H|\mathcal{O}_n(\mu_\Lambda)|H\rangle,\end{aligned} \tag{5}$$

where LH represents all possible light hadronic final states, and the operator $\mathcal{O}_n$ here and afterward only denotes the one relevant to the strong annihilation of $Q\bar{Q}$. The NR normalization has been applied for the state $|H\rangle$ in (5).

In order to calculate the coefficients of the four-fermion operators in (5), the equivalence of full QCD and NRQCD at long distance is exploited. Since in construction, the coefficient f_n is of a short-distance nature and is independent on the long-distance asymptotic state, one can get it by replacing the state $|H\rangle$ by the on-shell heavy quark pair state $|Q\bar{Q}\rangle$, with small relative momentum and matching the forward scattering amplitude of $Q\bar{Q} \to Q\bar{Q}$ in full QCD onto that of NRQCD perturbatively. The matching condition is written as [1]

$$\begin{aligned}\mathcal{A}(Q\bar{Q} \to Q\bar{Q})|_{\rm pertQCD} = {} & \sum_n \frac{f_n(\mu_\Lambda)}{m_Q^{d_n-4}} \\ & \times \langle Q\bar{Q}|\mathcal{O}_n(\mu_\Lambda)|Q\bar{Q}\rangle|_{\rm pertNRQCD}.\end{aligned} \tag{6}$$

[1]Here, v denotes the relative velocity of the heavy quark pair in the meson frame. The average value of v^2 is about 0.3 for charmonium and about 0.1 for bottomonium [1].

Since we only need the imaginary parts of the coefficients, the optical theorem can be used to simplify the matching calculations.

The physical $^1D_2$ state can be expanded in powers of v in the Fock space

$$|^1D_2\rangle = \mathcal{O}(1)|Q\bar{Q}(^1D_2^{[1]})\rangle + \mathcal{O}(v)|Q\bar{Q}(^1P_1^{[8]})\rangle + \mathcal{O}(v^2)|Q\bar{Q}(^1S_0^{[1,8]})\rangle + \ldots, \tag{7}$$

where the superindices [1,8] denote the color-singlet and color-octet, respectively. The contributions from the P-wave and S-wave Fock states to the annihilation rate of $^1D_2$ are at the same order of v^2 as that from the D-wave state, because their relevant operators scale v^{-2} and v^{-4} relative to $\mathcal{O}_1(^1D_2)$, as can be seen later. Other Fock states contribute at the higher order of v^2. Therefore, the light hadronic decay width of $^1D_2$ at leading order in v^2 can be described in NRQCD factorization framework as follows:

$$\begin{aligned}\Gamma(^1D_2 \to LH) = {} & 2\,\mathrm{Im} f(^1D_2^{[1]})\frac{\langle ^1D_2|\mathcal{O}_1(^1D_2)|^1D_2\rangle}{m_Q^6} \\ & + 2\,\mathrm{Im} f(^1P_1^{[8]})\frac{\langle ^1D_2|\mathcal{O}_8(^1P_1)|^1D_2\rangle}{m_Q^4} \\ & + 2\,\mathrm{Im} f(^1S_0^{[8]})\frac{\langle ^1D_2|\mathcal{O}_8(^1S_0)|^1D_2\rangle}{m_Q^2} \\ & + 2\,\mathrm{Im} f(^1S_0^{[1]})\frac{\langle ^1D_2|\mathcal{O}_1(^1S_0)|^1D_2\rangle}{m_Q^2},\end{aligned} \tag{8}$$

where the four-fermion operators are [20,21]

$$\begin{aligned}\mathcal{O}_1(^1S_0) &= \frac{1}{2N_c}\psi^\dagger\chi\chi^\dagger\psi, \\ \mathcal{O}_8(^1S_0) &= \psi^\dagger T^a\chi\chi^\dagger T^a\psi, \\ \mathcal{O}_8(^1P_1) &= \psi^\dagger\Big(-\frac{i}{2}\overleftrightarrow{\boldsymbol{D}}\Big)T^a\chi\cdot\chi^\dagger(-\frac{i}{2}\overleftrightarrow{\boldsymbol{D}}\mathbf{D})T^a\psi, \\ \mathcal{O}_1(^1D_2) &= \frac{1}{2N_c}\psi^\dagger S^{ij}\chi\chi^\dagger S^{ij}\psi,\end{aligned} \tag{9}$$

where $\overleftrightarrow{\boldsymbol{D}} = \overrightarrow{\boldsymbol{D}} - \overleftarrow{\boldsymbol{D}}$ and $S^{ij} = (-\frac{i}{2})^2(\overleftrightarrow{D}^i\overleftrightarrow{D}^j - \frac{1}{3}\overleftrightarrow{\boldsymbol{D}}^2\delta^{ij})$. Since $\boldsymbol{D}^2/m_Q^2$ scales as v^2, it can be ensured that the four terms in (47) are at the same order of v.

The coefficients in (47) can be obtained by applying the matching conditions (6) to appropriate $Q\bar{Q}$ configurations. To subtract the full QCD amplitude of $Q\bar{Q}$ state of a particular angular momentum, the covariant projection method is adopted. In practice, the optical theorem can relate the imaginary part of the QCD amplitude $\mathcal{A}$ in (6) to the parton-level decay width [20,22]

$$\Gamma(Q\bar{Q}[n] \to LFs) = \frac{1}{2M}\langle Q\bar{Q}[n]|\mathcal{O}[n]|Q\bar{Q}[n]\rangle_{NR}^{LO} \times \bar{\sum}\int|\mathcal{M}(Q\bar{Q}[n] \to LFs)|^2 d\Phi, \tag{10}$$

where LFs denote the gluons or light quarks and $[n]$ denotes the configuration of the $Q\bar{Q}$. The state $|Q\bar{Q}[n]\rangle$ has been normalized relativistically as one composite state with mass $M = 2E_Q$, except that in the matrix element in (10), where the state is normalized nonrelativistically to match the results in perturbative NRQCD conveniently. The superindex LO of the matrix element means that it is evaluated at tree level, and we always use the abbreviation $\langle\mathcal{O}[n]\rangle_{\mathrm{LO}}$ to represent it in our calculations. Moreover, the summation/average of the color and polarization for the final/initial state has been implied by the symbol $\bar{\sum}$.

For spin-singlet states with $L = 0$, $L = 1$ and $L = 2$, the amplitudes $\mathcal{M}$ defined in (10) are given by [22]

$$\begin{aligned}\mathcal{M}((Q\bar{Q})_{^1S_0}^{[1,8]} \to LFs) &= \sqrt{\frac{2}{M}}\mathrm{Tr}[\mathcal{C}^{[1,8]}\Pi^0\mathcal{M}^{am}]|_{q=0}, \\ \mathcal{M}((Q\bar{Q})_{^1P_1}^{[8]} \to LFs) &= \epsilon_\alpha^{[P]}\sqrt{\frac{2}{M}}\frac{d}{dq_\alpha}\mathrm{Tr}[\mathcal{C}^{[8]}\Pi^0\mathcal{M}^{am}]|_{q=0}, \\ \mathcal{M}((Q\bar{Q})_{^1D_2}^{[1]} \to LFs) &= \frac{1}{2}\epsilon_{\alpha\beta}^{[D]}\sqrt{\frac{2}{M}}\frac{d^2}{dq_\alpha dq_\beta} \times \mathrm{Tr}[\mathcal{C}^{[1]}\Pi^0\mathcal{M}^{am}]|_{q=0},\end{aligned} \tag{11}$$

where $\mathcal{M}^{am}$ denotes the parton-level amplitude amputated of the heavy quark spinors, and $\epsilon_\alpha^{[P]}$ and $\epsilon_{\alpha\beta}^{[D]}$ are the polarization tensors for the $L = P$, D states, respectively. The factor $\sqrt{\frac{2}{M}} = \frac{\sqrt{2M}}{\sqrt{2E_Q}\sqrt{2E_{\bar{Q}}}}$ comes from the normalization of the composite state $|Q\bar{Q}[n]\rangle$. For the color-singlet and octet states, the color projectors are $\mathcal{C}^{[1]} = \frac{\delta_{ij}}{\sqrt{N_c}}$ and $\mathcal{C}^{[8]} = \sqrt{2}(T_a)_{ij}$, respectively [22]. The covariant spin-singlet projector Π^0 in (11) is defined by

$$\Pi^0 = \sum_{s\bar{s}} u(s)\bar{v}(\bar{s})\Big\langle\frac{1}{2}, s; \frac{1}{2}, \bar{s}\,\Big|\,0, 0\Big\rangle. \tag{12}$$

The explicit form of Π^0 in D dimensions will be discussed in the next subsection.

The sums over polarization tensors for $\epsilon_\alpha^{[P]}$ and $\epsilon_{\alpha\beta}^{[D]}$ in D dimensions are

$$\sum_{J_z}\epsilon_\alpha^{[P]}\epsilon_{\alpha'}^{[P]*} = \Pi_{\alpha\alpha'}, \tag{13a}$$

$$\sum_{J_z}\epsilon_{\alpha\beta}^{[D]}\epsilon_{\alpha'\beta'}^{[D]*} = \frac{1}{2}(\Pi_{\alpha\alpha'}\Pi_{\beta\beta'} + \Pi_{\alpha\beta'}\Pi_{\alpha'\beta}) - \frac{1}{D-1}\Pi_{\alpha\beta}\Pi_{\alpha'\beta'}. \tag{13b}$$

Here, $\Pi_{\alpha\alpha'}$ is defined as

$$\Pi_{\alpha\alpha'} = -g_{\alpha\alpha'} + \frac{P_\alpha P_{\alpha'}}{M^2}, \tag{14}$$

where P is the total momentum of $Q\bar{Q}$, and $P^2 = M^2 = 4E_Q^2$.

Needless to say, the final result should be independent on the normalization convention of the $Q\bar{Q}$ state. If one wants to apply NR normalization thoroughly in the calculations, one needs to eliminate the factors $1/(2M)$ in (10) and $\sqrt{2/M}$ in (11), and then to replace the covariant spinors in (12) with the NR ones with the normalization condition $u^\dagger u = v^\dagger v = 1$.

A. Discussions on γ^5 scheme and projection operator

We will do our calculations in a dimensional regularization scheme both for QCD and NRQCD. Since we are only dealing with the spin-singlet Fock states, there will be the problem of definition of γ^5 in D dimensions. In our calculation, the γ^5 matrix can be represented as [23]

$$\gamma^5 = -\frac{i}{4!}\epsilon^{\mu\nu\rho\sigma}\gamma_\mu\gamma_\nu\gamma_\rho\gamma_\sigma. \tag{15}$$

The calculation involving γ^5 is carried out in D dimensions, where $\epsilon^{\mu\nu\rho\sigma}$ and γ^μ are all defined in D dimensions. Our prescription of γ^5 is equivalent to the naive γ^5 scheme for processes where each closed fermion chain contains at most one γ^5. Other prescriptions may be found in the literature [24–27].

In four dimensions, the covariant spin-singlet projector Π^0 defined in (12) can be given by (see, e.g., [28])

$$\Pi^0 = \frac{1}{2\sqrt{2}(E_Q + m_Q)}\left(\frac{\not{P}}{2} + \not{q} + m_Q\right)\frac{(\not{P} + M)}{M} \times \gamma^5\left(\frac{\not{P}}{2} - \not{q} - m_Q\right), \tag{16}$$

where q is half of the relative momentum of the heavy quark pair. The form in (16) cannot keep **C** parity conservation in D dimensions because $(\not{P} + M)\gamma^5$ cannot keep an invariant form under charge conjugation transformation in $D \neq 4$ dimensions. This problem can be solved by replacing it by the following two operators: For spin-singlet states the spin projectors of incoming heavy quark pairs at any order in v^2 are given by

$$\Pi^0 = \frac{1}{2\sqrt{2}(E_Q + m_Q)}\left(\frac{\not{P}}{2} + \not{q} + m_Q\right) \times \frac{[(\not{P} + M)\gamma^5 + \gamma^5(-\not{P} + M)]}{2M}\left(\frac{\not{P}}{2} - \not{q} - m_Q\right) \tag{17}$$

from [29] and

$$\Pi^0 = \frac{1}{2\sqrt{2}(E_Q + m_Q)}\left(\frac{\not{P}}{2} + \not{q} + m_Q\right) \times \frac{(\not{P} + M)\gamma^5(-\not{P} + M)}{2M^2}\left(\frac{\not{P}}{2} - \not{q} - m_Q\right) \tag{18}$$

from [30]. The above two projection operators both give correct results and keep **C** parity conservation.

III. FULL QCD CALCULATION

In this section, we calculate the imaginary part of $Q\bar{Q}$ forward scattering amplitude, or equivalently, the parton-level decay width Γ defined in (10). In the calculation, we use FEYNARTS [31] to generate the Feynman diagrams and amplitudes and FEYNCALC [32] for the tensor reduction. We regularize the ultraviolet (UV) and infrared (IR) divergence in dimensional regularization scheme and extend the covariant projection method into $D = 4 - 2\epsilon$ dimensions as has been mentioned.

The leading order subprocesses in α_s are the annihilations of $Q\bar{Q}[n]$ into two gluons, where n can be any configurations of the Fock states listed in (7). The Feynman diagrams at LO of α_s are shown in Fig. 1. And the results in D dimensions are

$$\begin{aligned}
\Gamma_{\text{Born}}({}^1S_0^{[1]} \to gg) &= \frac{C_F\alpha_s^2 16\pi^2}{m_Q^2}\Phi_2(1-\epsilon)(1-2\epsilon)\langle\mathcal{O}({}^1S_0^{[1]})\rangle_{\text{LO}},\\
\Gamma_{\text{Born}}({}^1S_0^{[8]} \to gg) &= \frac{B_F\alpha_s^2 16\pi^2}{m_Q^2}\Phi_2(1-\epsilon)(1-2\epsilon)\langle\mathcal{O}({}^1S_0^{[8]})\rangle_{\text{LO}},\\
\Gamma_{\text{Born}}({}^1P_1^{[8]} \to gg) &= \frac{C_A\alpha_s^2 4\pi^2}{m_Q^4}\Phi_2\frac{(1-\epsilon)(1-2\epsilon)}{3-2\epsilon}\langle\mathcal{O}({}^1P_1^{[8]})\rangle_{\text{LO}},\\
\Gamma_{\text{Born}}({}^1D_2^{[1]} \to gg) &= \frac{C_F\alpha_s^2 4\pi^2}{m_Q^6}\Phi_2\frac{(1-2\epsilon)(6\epsilon^2-15\epsilon+8)}{4\epsilon^2-16\epsilon+15}\langle\mathcal{O}({}^1D_2^{[1]})\rangle_{\text{LO}},
\end{aligned} \tag{19}$$

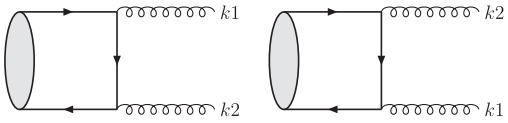

FIG. 1. Feynman diagrams for ${}^1L_J^{[1,8]} \to gg$.

where $B_F = \frac{N_c^2-4}{4N_c} = \frac{5}{12}$, and $\Phi_{(2)}$ is the two-body phase space in D dimensions: $\frac{1}{8\pi}\frac{\Gamma(1-\epsilon)}{\Gamma(2-2\epsilon)}(\frac{\pi}{m_Q^2})^\epsilon$. The first three results in (19) are consistent with those in Refs. [20,22]. At the Born level, there are no IR divergences in the results since both the two gluons should be hard in the rest frame of $Q\bar{Q}$.

A. Real corrections

The real corrections to Born level subprocesses include the decays into ggg and $q\bar{q}g$ final states. The corresponding Feynman diagrams are shown in Figs. 2 and 3. For simplicity, unphysical polarization summation is used for final state gluons, so diagrams with ghosts in the final states must be included in the calculation when a three gluon vertex appears, in order to cancel the nonphysical degrees of freedom to keep the full results gauge invariant.

1. $(Q\bar{Q})_{1L_J^{[1,8]}} \to ggg$

Our results of S-wave configurations agree with those in [20,22] and are listed below:

$$\Gamma({}^1S_0^{[1]} \to ggg) = \frac{C_A\alpha_s}{\pi}\Gamma_{\rm Born}({}^1S_0^{[1]} \to gg) f_\epsilon(M^2) \times \left(\frac{1}{\epsilon^2} + \frac{11}{6\epsilon} + \frac{181}{18} - \frac{23}{24}\pi^2\right),$$
$$\Gamma({}^1S_0^{[8]} \to ggg) = \frac{C_A\alpha_s}{\pi}\Gamma_{\rm Born}({}^1S_0^{[8]} \to gg) f_\epsilon(M^2) \times \left(\frac{1}{\epsilon^2} + \frac{7}{3\epsilon} + \frac{104}{9} - \pi^2\right), \quad (20)$$

where $f_\epsilon(M^2) = (\frac{4\pi\mu^2}{M^2})^\epsilon\Gamma(1+\epsilon)$. The D-dimension P and D-wave results are

$$\Gamma({}^1P_1^{[8]} \to ggg) = \frac{C_A\alpha_s}{\pi}\Gamma_{\rm Born}({}^1P_1^{[8]} \to gg) f_\epsilon(M^2) \times \left(\frac{1}{\epsilon^2} + \frac{71}{27\epsilon} + \frac{7(-168+25\pi^2)}{162}\right),$$
$$\Gamma({}^1D_2^{[1]} \to ggg) = \frac{C_A\alpha_s}{\pi}\Gamma_{\rm Born}({}^1D_2^{[1]} \to gg) f_\epsilon(M^2) \times \left(\frac{1}{\epsilon^2} + \frac{3}{\epsilon} + \frac{7027}{144} - \frac{277}{64}\pi^2\right). \quad (21)$$

Both soft and collinear IR divergences are there in the results in (20) and (21), and the square pole $1/\epsilon^2$ comes from the overlap of the soft and the collinear regions.

2. $(Q\bar{Q})_{1L_J^{[1,8]}} \to q\bar{q}g$

Another subprocess of light hadronic decay is to $q\bar{q}g$ final states, and only two graphs make contribution to this subprocess (shown in Fig. 3).

We get the following results:

$$\Gamma({}^1S_0^{[1]} \to q\bar{q}g) = N_f\Gamma_{\rm Born}({}^1S_0^{[1]} \to gg)\frac{\alpha_s}{\pi}\frac{f_\epsilon(M^2)}{K}T_F\left(-\frac{2}{3\epsilon} - \frac{16}{9}\right),$$
$$\Gamma({}^1S_0^{[8]} \to q\bar{q}g) = N_f\Gamma_{\rm Born}({}^1S_0^{[8]} \to gg)\frac{\alpha_s}{\pi}\frac{f_\epsilon(M^2)}{K}T_F\left(-\frac{2}{3\epsilon} - \frac{16}{9}\right),$$
$$\Gamma({}^1P_1^{[8]} \to q\bar{q}g) = N_f\Gamma_{\rm Born}({}^1P_1^{[8]} \to gg)\frac{\alpha_s}{\pi}\frac{f_\epsilon(M^2)}{K}T_F\left(-\frac{2}{3\epsilon} - \frac{16}{9}\right),$$
$$\Gamma({}^1D_2^{[1]} \to q\bar{q}g) = N_f\Gamma_{\rm Born}({}^1D_2^{[1]} \to gg)\frac{\alpha_s}{\pi}\frac{f_\epsilon(M^2)}{K}T_F\left(-\frac{2}{3\epsilon} - \frac{16}{9}\right), \quad (22)$$

where N_f is the number of light flavor quarks. $N_f = 3$ and 4 for charmonium and bottomonium, respectively. $T_F = 1/2$, $K = \Gamma(1+\epsilon)\Gamma(1-\epsilon) \simeq 1 + \epsilon^2\frac{\pi^2}{6}$, and the S-wave results agree with [20,22].

There are only single poles of ϵ in the results in (22), and they can be identified as collinear ones. The absence of the soft IR divergence can be seen from the diagrams in Fig. 3. When the momentum of the real gluon goes to zero, it will decouple

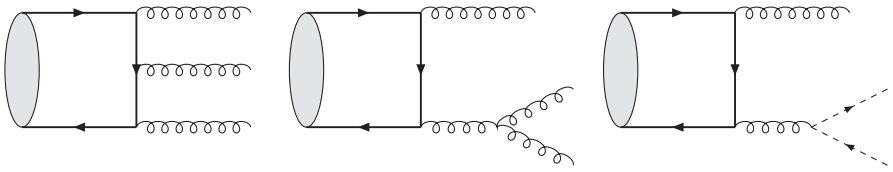

FIG. 2. Feynman diagrams for ${}^1L_J^{[1,8]} \to ggg$.

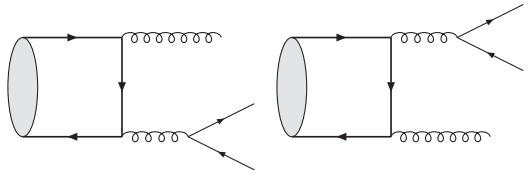

FIG. 3. Feynman diagrams for ${}^1L_J^{[1,8]} \to q\bar{q}g$.

from the quark line as an eikonal factor [20], then the results will be zero since $Q\bar{Q}$ in spin singlet cannot couple to one virtual gluon.

As will be seen later, the collinear divergences and partial soft IR ones in (20)–(22) are canceled by the virtual corrections to the Born level decay width. The remaining soft IR divergences are those in $\Gamma({}^1P_1^{[8]} \to ggg)$ and $\Gamma({}^1D_2^{[1]} \to ggg)$ from the first diagram in Fig. 2, which will be absorbed in the renormalization of the operators $\mathcal{O}_{1,8}({}^1S_0)$ and $\mathcal{O}_8({}^1P_1)$ in perturbative NRQCD. These are just the general results of the so-called topological factorization discussed in [1].

B. Virtual corrections

There are 23 virtual correction diagrams, including counterterm diagrams, divided into 9 groups. Representative Feynman diagrams of each class are shown in Fig. 4. And the others can be found through reversing the arrows on the quark lines or exchanging the final state gluons. UV divergences are removed by renormalization. The definitions of the renormalization constant of QCD gauge coupling constant $g_s = \sqrt{4\pi\alpha_s}$, heavy quark mass m_Q, heavy quark field ψ_Q, light quark field ψ_q, and gluon field A_μ are

$$g_s^0 = Z_g g_s, \qquad m_Q^0 = Z_{m_Q} m_Q, \qquad \psi_Q^0 = \sqrt{Z_{2Q}}\psi_Q,$$
$$\psi_q^0 = \sqrt{Z_{2q}}\psi_q, \qquad A_\mu^0 = \sqrt{Z_3}A_\mu, \tag{23}$$

where the superscript 0 labels bare quantities, and $Z_i = 1 + \delta Z_i$. The renormalized constant Z_g is defined by minimal-subtraction ($\overline{MS}$) scheme, and the others by the on-mass-shell (OS) scheme, similar to that in [33]. Then the results are

$$\begin{aligned}
\delta Z_{2Q}^{OS} &= -C_F \frac{\alpha_s}{4\pi} f_\epsilon(M^2)\left(\frac{1}{\epsilon_{UV}} + \frac{2}{\epsilon} + 6\ln(2) + 4\right),\\
\delta Z_{2q}^{OS} &= -C_F \frac{\alpha_s}{4\pi} f_\epsilon(M^2)\left(\frac{1}{\epsilon_{UV}} - \frac{1}{\epsilon}\right),\\
\delta Z_3^{OS} &= (b_0 - C_A)\frac{\alpha_s}{4\pi} f_\epsilon(M^2)\left(\frac{2}{\epsilon_{UV}} - \frac{2}{\epsilon}\right),\\
\delta Z_{m_Q}^{OS} &= -3C_F \frac{\alpha_s}{4\pi} f_\epsilon(M^2)\left(\frac{1}{\epsilon_{UV}} + 2\ln(2) + \frac{4}{3}\right),\\
\delta Z_g^{\overline{MS}} &= -b_0 \frac{\alpha_s}{4\pi} f_\epsilon(M^2)\left(\frac{1}{\epsilon_{UV}} - \ln\left(\frac{\mu^2}{4m_Q^2}\right)\right),
\end{aligned} \tag{24}$$

where $b_0 = \frac{11C_A}{6} - \frac{N_f}{3}$.

We calculate diagrams one by one and summarize the results in the following form:

$$\Gamma({}^1L_J^{[1,8]} \to gg)_{VC} = \Gamma({}^1L_J^{[1,8]} \to gg)_{\text{Born}} \frac{\alpha_s}{\pi} f_\epsilon(M^2) \times \sum_k \mathcal{D}_k, \tag{25}$$

where the results of $\mathcal{D}_k$ are listed in Tables I, II, III, and IV. We add the counterterm diagrams with the corresponding self-energy and vertex diagrams to show the explicit cancellation of the UV divergence. There are still IR diver-

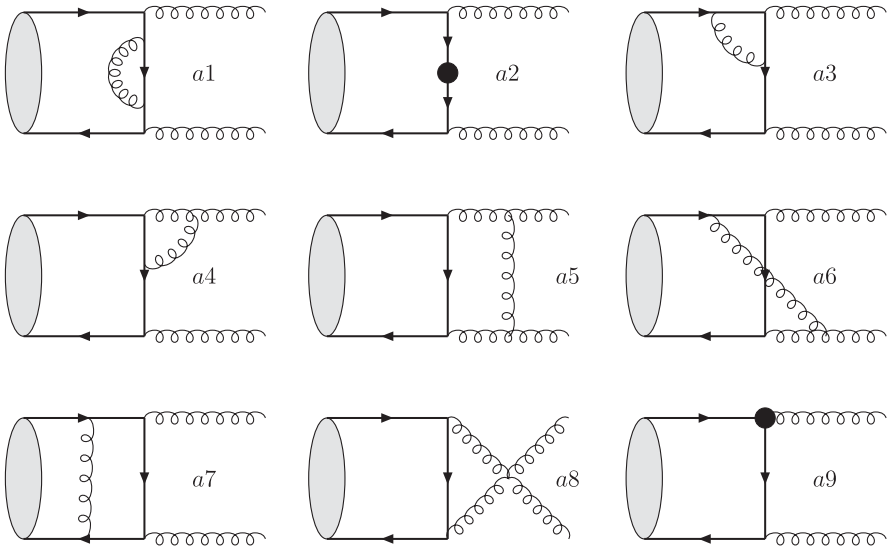

FIG. 4. One-loop Feynman diagrams for $(Q\bar{Q})_{{}^1L_J^{[1,8]}} \to gg$.

TABLE I. Virtual corrections to $(Q\bar{Q})_{1S_0^{[1]}} \to gg$.

Diag.	$\mathcal{D}_k$
a1 + a2	$C_F(\frac{1}{\epsilon}+1+6\ln 2)$
a3 + a4 + a9	$-\frac{C_A}{2\epsilon^2}+\frac{1}{\epsilon}(-2C_F-b_0+\frac{C_A}{2})+b_0\ln\frac{\mu^2}{4m_Q^2}+C_F(-8\ln 2-4+\frac{\pi^2}{4})-\frac{C_A}{2}(-4+\frac{\pi^2}{12})$
a5	$C_A(-\frac{1}{\epsilon^2}-\frac{1}{\epsilon}-2+2\ln 2+\frac{2}{3}\pi^2)$
a6	$\frac{1}{2}C_A(\frac{1}{\epsilon^2}+\frac{1}{\epsilon}+2-4\ln 2-\frac{5}{12}\pi^2)$
a7	$C_F(\frac{\pi^2}{2v}+\frac{1}{\epsilon}-2+2\ln 2)$
a8	0

gences left, which will be canceled by those in the real corrections as we have mentioned. There are also the well-known Coulomb singularities, which have been regularized by the relative velocity v, in Tables I, II, III, and IV. These singularities can be absorbed by the corresponding matrix element through the matching condition (6).

C. Summary of the QCD results

Combining the real and virtual correction results together and translating the parton-level decay width back to the imaginary part of the forward scattering amplitude, we get the full QCD results up to $\mathcal{O}(\alpha_s^3)$:

$$(2\,\mathrm{Im}\mathcal{A}(Q\bar{Q}[^1S_0^{[1]}]\to Q\bar{Q}[^1S_0^{[1]}]))|_{\mathrm{pertQCD}} = \left\{\frac{8\pi\alpha_s^2}{3m_Q^2}\left(1+\frac{2\pi\alpha_s}{3v}\right)+\frac{\alpha_s^3}{27m_Q^2}\left[4(477-16N_f)+12(33-2N_f)\ln\frac{\mu^2}{4m_Q^2}-93\pi^2\right]\right\}\langle\mathcal{O}(^1S_0^{[1]})\rangle_{\mathrm{LO}}, \tag{26a}$$

$$(2\,\mathrm{Im}\mathcal{A}(Q\bar{Q}[^1S_0^{[8]}]\to Q\bar{Q}[^1S_0^{[8]}]))|_{\mathrm{pertQCD}} = \left\{\frac{5\pi\alpha_s^2}{6m_Q^2}\left(1-\frac{\pi\alpha_s}{12v}\right)+\frac{5\alpha_s^3}{432m_Q^2}\left[16(153-4N_f)+12(33-2N_f)\ln\frac{\mu^2}{4m_Q^2}-129\pi^2\right]\right\}\langle\mathcal{O}(^1S_0^{[8]})\rangle_{LO}, \tag{26b}$$

$$(2\,\mathrm{Im}\mathcal{A}(Q\bar{Q}[^1P_1^{[8]}]\to Q\bar{Q}[^1P_1^{[8]}]))|_{\mathrm{pertQCD}} = \left\{\frac{\pi\alpha_s^2}{2m_Q^4}\left(1-\frac{\pi\alpha_s}{12v}\right)-\frac{19\alpha_s^3}{18m_Q^4}\left[\frac{1}{\epsilon}-\gamma_E+\ln(4\pi)\right]+\frac{\alpha_s^3[2(3(-8N_f-21\ln(2)-229)+119\pi^2)-3(6N_f-61)\ln(\frac{\mu^2}{4m_Q^2})]}{108m_Q^4}\right\}\times\langle\mathcal{O}(^1P_1^{[8]})\rangle_{LO}, \tag{26c}$$

$$(2\,\mathrm{Im}\mathcal{A}(Q\bar{Q}[^1D_2^{[1]}]\to Q\bar{Q}[^1D_2^{[1]}]))|_{\mathrm{pertQCD}} = \left\{\frac{16\pi\alpha_s^2}{45m_Q^6}\left(1+\frac{2\pi\alpha_s}{3v}\right)-\frac{8\alpha_s^3}{9m_Q^6}\left[\frac{1}{\epsilon}-\gamma_E+\ln(4\pi)\right]-\frac{\alpha_s^3[4(128N_f+1008\ln(2)-19509)+192(N_f-9)\ln(\frac{\mu^2}{4m_Q^2})+7263\pi^2]}{1620m_Q^6}\right\}\times\langle\mathcal{O}(^1D_2^{[1]})\rangle_{LO}, \tag{26d}$$

TABLE II. Virtual corrections to $(Q\bar{Q})_{1S_0^{[8]}} \to gg$.

Diag.	$\mathcal{D}_k$
a1 + a2	$C_F(\frac{1}{\epsilon}+1+6\ln 2)$
a3 + a4 + a9	$-\frac{C_A}{2\epsilon^2}+\frac{1}{\epsilon}(-2C_F-b_0+\frac{C_A}{2})+b_0\ln\frac{\mu^2}{4m_Q^2}+C_F(-8\ln 2-4+\frac{\pi^2}{4})-\frac{C_A}{2}(-4+\frac{\pi^2}{12})$
a5	$\frac{1}{2}C_A(-\frac{1}{\epsilon^2}-\frac{1}{\epsilon}-2+2\ln 2+\frac{2}{3}\pi^2)$
a6	0
a7	$(C_F-\frac{1}{2}C_A)(\frac{\pi^2}{2v}+\frac{1}{\epsilon}-2+2\ln 2)$
a8	0

TABLE III. Virtual corrections to $(Q\bar{Q})_{1P_1^{[8]}} \to gg$.

Diag.	$\mathcal{D}_k$
a1 + a2	$C_F(\frac{1}{\epsilon} - 3 + 10\ln 2)$
a3 + a4 + a9	$-\frac{C_A}{2\epsilon^2} - \frac{1}{\epsilon}(2C_F + b_0 + \frac{C_A}{2}) + b_0 \ln\frac{\mu^2}{4m_Q^2} + C_F(\frac{\pi^2}{2} - 16\ln 2) - \frac{C_A}{2}(-6 + \frac{\pi^2}{3} + 2\ln 2)$
a5	$\frac{1}{2}C_A(-\frac{1}{\epsilon^2} - \frac{1}{\epsilon} - 5 + \frac{2}{3}\pi^2 + 5\ln 2)$
a6	0
a7	$(C_F - \frac{1}{2}C_A)(\frac{\pi^2}{2v} + \frac{1}{\epsilon} - 2 + 2\ln 2)$
a8	$C_A(-\frac{1}{2} + \frac{\ln 2}{2})$

TABLE IV. Virtual corrections to $(Q\bar{Q})_{1D_2^{[1]}} \to gg$.

Diag.	$\mathcal{D}_k$
a1 + a2	$C_F(\frac{1}{\epsilon} - 10 + 22\ln 2)$
a3 + a4 + a9	$-\frac{C_A}{2\epsilon^2} - \frac{1}{\epsilon}(2C_F + b_0 + C_A) + b_0 \ln\frac{\mu^2}{4m_Q^2} + C_F(10 + \frac{3}{4}\pi^2 - 38\ln 2) - \frac{C_A}{2}(-\frac{15}{8} + \frac{7}{12}\pi^2 + 2\ln 2)$
a5	$C_A(-\frac{1}{\epsilon^2} - \frac{1}{\epsilon} - 8 + \frac{2}{3}\pi^2 + 12\ln 2)$
a6	$\frac{1}{2}C_A(\frac{1}{\epsilon^2} + \frac{69}{8} - \frac{7}{6}\pi^2 - 16\ln 2)$
a7	$C_F(\frac{\pi^2}{2v} + \frac{1}{\epsilon} - 2 + 4\ln 2)$
a8	0

where the states $|Q\bar{Q}[n]\rangle$ in the left-hand side and the right-hand side should be understood to have been normalized under the same condition. Moreover, the equalities in (26) are independent on the normalization conventions. That is, the state $|Q\bar{Q}[n]\rangle$ can be normalized either relativistically or nonrelativistically, either as a composite state or as a discrete state. Therefore, it is convenient to use $\mathrm{Im}\mathcal{A}$ to do the matching calculations, and we will use the abbreviation $\mathrm{Im}\mathcal{A}(n)$ to represent the amplitudes in (26).

The remaining infrared divergences and Coulomb singularities in (26) will be precisely repeated in the radiative corrections of the matrix elements in perturbative NRQCD in next section. The finite short-distance coefficients will be obtained after matching calculations.

IV. NRQCD RESULTS AND OPERATOR EVOLUTION EQUATIONS

In this section, we calculate the NRQCD corrections to the four-fermion operators in D dimensions. As we have mentioned, we will adopt the method of regions [19] to avoid the mismatch of the loop momenta in different regions. Furthermore, each loop integral in this method contributes only to a single power in v, thus one can do the power counting before the integral has been explicitly done.

Since the ultrasoft and the QCD scale are comparable, $m_Q v^2 \sim \Lambda_{\mathrm{QCD}}$, for both charmonium and bottomonium, there are only two low-energy scales to be considered in NRQCD, which satisfy the inequality $m_Q v \gg m_Q v^2$. Thus, the nontrivial contributions to the NRQCD loop integrals come only from the following three regions:

$$\begin{aligned}
\text{soft: } A_s^\mu &: k_0 \sim |\vec{k}| \sim m_Q v, \\
\Psi_s &: T \sim |\vec{p}| \sim m_Q v, \\
\text{potential: } A_p^\mu &: k_0 \sim m_Q v^2, |\vec{k}| \sim m_Q v, \\
\Psi_p &: T \sim m_Q v^2, |\vec{p}| \sim m_Q v, \\
\text{ultrasoft: } A_u^\mu &: k_0 \sim |\vec{k}| \sim m_Q v^2,
\end{aligned} \tag{27}$$

where k_ν and p_ν are the momenta of gluon field and heavy quark field, respectively, and $T = p_0 - m_Q$. The loop momenta running in these regions scale as those of the corresponding gluons in dimensional regularization scheme. One can check that the other regions, such as that with $k_0 \sim m_Q v$ and $\vec{k} \sim m_Q v^2$, have no contributions to the NRQCD loop integrals in the dimensional regularization scheme. From the view point of effective field theory, the five modes defined in (27) can be all treated as the effective fields in NRQCD. Only after parting these

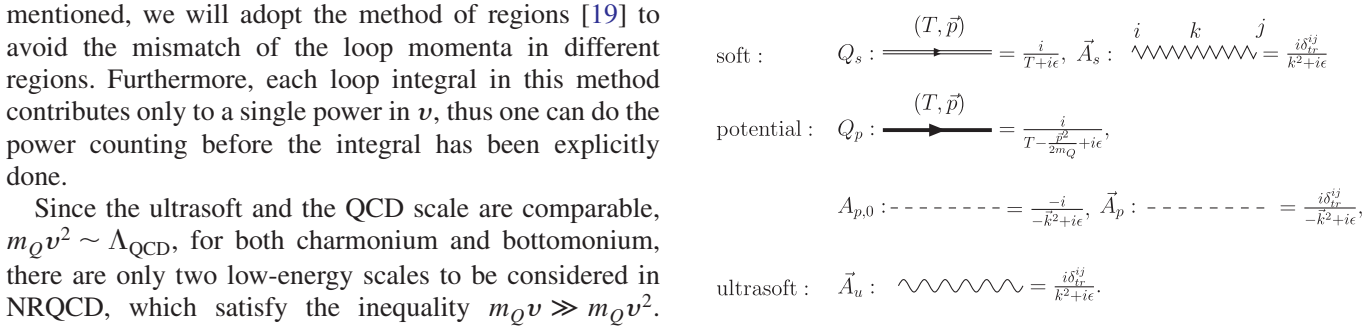

FIG. 5. NRQCD Feynman rules for heavy quark and gluon propagators in different regions.

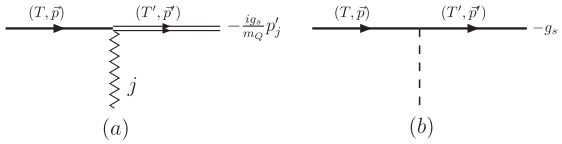

FIG. 6. NRQCD Feynman rules for heavy quark and gluon vertices.

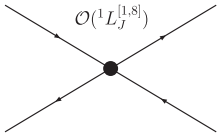

FIG. 7. NRQCD Feynman diagrams for LO Matrix Elements.

low-energy modes sufficiently like what has been done in (27), the homogeneous power counting rules can be gotten.

In practice, we use the NRQCD Feynman rules [34] derived in Coulomb gauge for the three regions (or the five low-energy modes) in our calculations. These rules are shown in Figs. 5 and 6, where $\delta^{ij}_{tr} = \delta^{ij} - \frac{k^i k^j}{|\mathbf{k}|^2}$. The Feynman rules for antiheavy quark could be obtained by charge conjugation symmetry.

The Coulomb singularities calculated in the full QCD theory correspond to the potential region, while the soft divergences to the soft one. The LO Feynman diagrams for matrix elements are shown in Fig. 7. The on-shell external quark lines lie in potential region. At next-to-leading order (NLO) in α_s, only six classes of Feynman diagrams shown in Fig. 8 need to be calculated for our purpose [8]. The first four diagrams (a)–(d) have inner gluon lines connecting with one incoming quark line and one outgoing quark line, and the soft region will give the lowest order nontrivial result in v [8]. In the last two diagrams (e) and (f) the inner gluon line joints two incoming or outgoing quark lines, and only the potential region has nonvanishing real value [8]. The self-energy diagrams in the external legs are dropped in accordance with the on-shell renormalization scheme used in the full QCD calculation.

We present here the detailed calculation of the NLO correction to the P-wave octet operator $\mathcal{O}(^1P_1^{[8]})$. The LO result $\langle\mathcal{O}(^1P_1^{[8]})\rangle_{\rm Born}$ is trivial. Using the Feynman rules for propagators of heavy quark and gluon in soft region and for the heavy quark gluon vertex between potential and soft regions, the loop integral of diagram (a) is

$$I_a = \frac{ig_s^2}{m_Q^2}\int\frac{d^Dk}{(2\pi)^D}\frac{\mathbf{p}\cdot\mathbf{p}' - (\mathbf{p}\cdot\mathbf{k})(\mathbf{p}'\cdot\mathbf{k})/\mathbf{k}^2}{k_0^2 - \mathbf{k}^2 + i\epsilon} \times\frac{1}{k_0 - i\epsilon}\frac{1}{k_0 - i\epsilon}. \tag{28}$$

After performing the contour integration of $k_0 = |\mathbf{k}| - i\epsilon$, we get[2]

$$I_a = \frac{g_s^2}{2m_Q^2}\int\frac{d^{D-1}k}{(2\pi)^{D-1}}\frac{\mathbf{p}\cdot\mathbf{p}' - (\mathbf{p}\cdot\mathbf{k})(\mathbf{p}'\cdot\mathbf{k})/\mathbf{k}^2}{|\mathbf{k}|^3}, \tag{29}$$

which is both infrared and ultraviolet divergent. The integral in (29) is scaleless, so it vanishes in dimensional regularization. That is, the UV pole will be canceled by the IR one. But the result is nontrivial:

$$I_a = \frac{\alpha_s}{3\pi m_Q^2}\left(\frac{1}{\epsilon_{UV}} - \frac{1}{\epsilon}\right)\mathbf{p}\cdot\mathbf{p}'. \tag{30}$$

The integrals of (b)–(d) in Fig. 8 could be evaluated in the same way, and their results are

$$I_{b-d} = \frac{\alpha_s}{3\pi m_Q^2}\left(\frac{1}{\epsilon_{UV}} - \frac{1}{\epsilon}\right)\mathbf{p}\cdot\mathbf{p}'. \tag{31}$$

Making use of the Feynman rules for heavy quarks and gluon in potential region, we obtain the loop integral of diagram (e):

$$I_e = -ig_s^2\int\frac{d^Dk}{(2\pi)^D}\frac{1}{\mathbf{k}^2}\frac{1}{T + k_0 - \frac{(\mathbf{p}+\mathbf{k})^2}{2m_Q} + i\epsilon} \times\frac{1}{T - k_0 - \frac{(\mathbf{p}+\mathbf{k})^2}{2m_Q} + i\epsilon}, \tag{32}$$

where $T = \frac{|\mathbf{p}|^2}{2m_Q}$. Integrating k_0, we have

$$I_e = g_s^2 m_Q\int\frac{d^{D-1}k}{(2\pi)^{D-1}}\frac{1}{\mathbf{k}^2}\frac{1}{\mathbf{k}^2 + 2\mathbf{p}\cdot\mathbf{k} - i\epsilon}. \tag{33}$$

This integral could be performed directly by introducing $v = \frac{|\mathbf{p}|}{m_Q}$, and we get the Coulomb singularity

$$I_e = \frac{\alpha_s\pi}{4v}\left(1 - \frac{i}{\pi}\left(\frac{1}{\epsilon} - \ln\left(\frac{m_Q^2v^2}{\pi\mu^2}\right) - \gamma_E\right)\right). \tag{34}$$

The integral of diagram (f) gives the same Coulomb singularity but with opposite sign in the imaginary part.

The color structures of diagrams (a,c), (b,d), and (e,f) are obtained by color decomposition and are listed below, respectively:

$$\begin{aligned}
\sqrt{2}T^aT^b\otimes T^b\sqrt{2}T^a &= C_F\frac{1}{\sqrt{3}}\otimes\frac{1}{\sqrt{3}} + \frac{N_c^2-2}{2N_c}\sqrt{2}T^c\otimes\sqrt{2}T^c,\\
\sqrt{2}T^aT^b\otimes\sqrt{2}T^aT^b &= C_F\frac{1}{\sqrt{3}}\otimes\frac{1}{\sqrt{3}} + \frac{-2}{2N_c}\sqrt{2}T^c\otimes\sqrt{2}T^c,\\
T^b\sqrt{2}T^aT^b\otimes\sqrt{2}T^a &= \left(C_F - \frac{1}{2}C_A\right)\sqrt{2}T^c\otimes\sqrt{2}T^c.
\end{aligned} \tag{35}$$

Summing over each integral multiplied by the according color factor we get NRQCD matrix element of the P-wave operator at NLO, which is UV divergent and needs to be

[2]Since the quark propagator poles should be taken into account in the potential region, one only needs to evaluate the contribution from the gluon pole in the soft region [19].

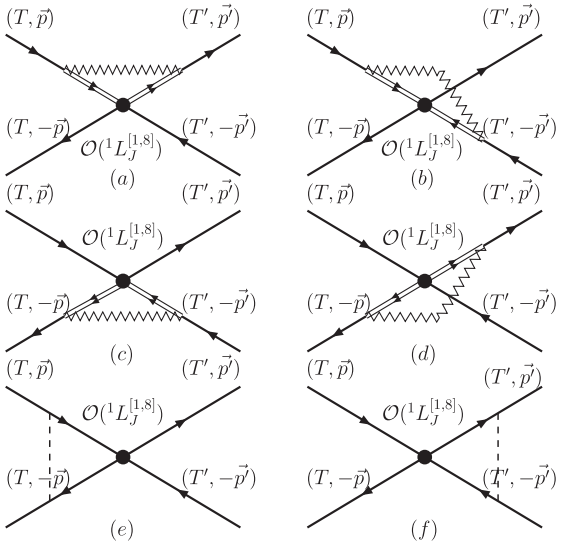

FIG. 8. NRQCD Feynman diagrams for NLO Matrix Elements.

renormalized:

$$\langle \mathcal{O}^0(^1P_1^{[8]})\rangle_{\rm NLO} = \left\{\left(1+\frac{\alpha_s\pi}{2v}\left(C_F-\frac{1}{2}C_A\right)\right)\sqrt{2}T^c\otimes\sqrt{2}T^c + \frac{4\alpha_s(\frac{\mu}{\mu_\Lambda})^{2\epsilon}}{3\pi m_Q^2}\left(\frac{1}{\epsilon_{UV}}-\frac{1}{\epsilon}\right)\left[C_F\frac{1}{\sqrt{3}}\otimes\frac{1}{\sqrt{3}} + B_F\sqrt{2}T^c\otimes\sqrt{2}T^c\right]\mathbf{p}\cdot\mathbf{p}'\right\}\langle\bar{\mathcal{O}}(^1P_1)\rangle_{\rm LO}, \tag{36}$$

where we have used $\langle \mathcal{O}^0(^1P_1^{[8]})\rangle = \langle\bar{\mathcal{O}}^0(^1P_1)\rangle\times\sqrt{2}T^a\otimes\sqrt{2}T^a$ and the superscript 0 means the bare operator. Before doing the operator renormalization, we first re-express the bare result as

$$\langle \mathcal{O}^0(^1P_1^{[8]})\rangle_{\rm NLO} = \left(1+\frac{\alpha_s\pi}{2v}\left(C_F-\frac{1}{2}C_A\right)\right)\langle\mathcal{O}(^1P_1^{[8]})\rangle_{\rm LO} + \frac{4\alpha_s(\frac{\mu}{\mu_\Lambda})^{2\epsilon}}{3\pi m_Q^2}\left(\frac{1}{\epsilon_{UV}}-\frac{1}{\epsilon}\right)\times(C_F\langle\mathcal{O}(^1D_2^{[1]})\rangle_{\rm LO}+B_F\langle\mathcal{O}(^1D_2^{[8]})\rangle_{\rm LO}). \tag{37}$$

From the above equation we can see that the color-octet P-wave operator is mixed with the color-singlet D-wave operator at NLO in α_s. We define the renormalized operator $\mathcal{O}^R(^1P_1^{[8]})$ through [33]

$$\langle \mathcal{O}^0(^1P_1^{[8]})\rangle_{\rm NLO} = \langle \mathcal{O}^R(^1P_1^{[8]})\rangle_{\rm NLO} + \frac{4\alpha_s(\frac{\mu}{\mu_\Lambda})^{2\epsilon}}{3\pi m_Q^2}\times\left(\frac{1}{\epsilon_{UV}}+\ln 4\pi-\gamma_E\right)(C_F\langle\mathcal{O}(^1D_2^{[1]})\rangle_{\rm LO} + B_F\langle\mathcal{O}(^1D_2^{[8]})\rangle_{\rm LO}). \tag{38}$$

Here, the $\overline{MS}$ renormalization scheme is adopted. The matrix element of the renormalized operator is UV finite, but still has an IR divergence term, which will cancel the infrared divergent D-wave full QCD result. And it also has the Coulomb singularity, which is the same as that appearing in the full QCD virtual correction:

$$\langle \mathcal{O}^R(^1P_1^{[8]})\rangle_{\rm NLO} = \left(1+\frac{\alpha_s\pi}{2v}\left(C_F-\frac{1}{2}C_A\right)\right)\langle\mathcal{O}(^1P_1^{[8]})\rangle_{\rm LO} + \frac{4\alpha_s(\frac{\mu}{\mu_\Lambda})^{2\epsilon}}{3\pi m_Q^2}\left(-\frac{1}{\epsilon}-\ln 4\pi+\gamma_E\right)\times(C_F\langle\mathcal{O}(^1D_2^{[1]})\rangle_{\rm LO}+B_F\langle\mathcal{O}(^1D_2^{[8]})\rangle_{\rm LO}). \tag{39}$$

Here, the matrix element of $\mathcal{O}(^1D_2^{[8]})$ is at higher order in v in our case and therefore can be eliminated. The matrix elements of S-wave singlet and octet operators and that of the D-wave singlet operator could be computed in the same way:

$$\langle \mathcal{O}^R(^1S_0^{[1]})\rangle_{\rm NLO} = \left(1+\frac{\alpha_s\pi}{2v}C_F\right)\langle\mathcal{O}(^1S_0^{[1]})\rangle_{\rm LO} + \frac{1}{2N_c}\frac{4\alpha_s(\frac{\mu}{\mu_\Lambda})^{2\epsilon}}{3\pi m_Q^2}\left(-\frac{1}{\epsilon}-\ln 4\pi+\gamma_E\right)\times\langle\mathcal{O}(^1P_1^{[8]})\rangle_{\rm LO}, \tag{40}$$

$$\langle \mathcal{O}^R(^1S_0^{[8]})\rangle_{\rm NLO} = \left(1+\frac{\alpha_s\pi}{2v}\left(C_F-\frac{1}{2}C_A\right)\right)\langle\mathcal{O}(^1S_0^{[8]})\rangle_{\rm LO} + B_F\frac{4\alpha_s(\frac{\mu}{\mu_\Lambda})^{2\epsilon}}{3\pi m_Q^2}\left(-\frac{1}{\epsilon}-\ln 4\pi+\gamma_E\right)\times\langle\mathcal{O}(^1P_1^{[8]}\rangle_{\rm LO}+\ldots, \tag{41}$$

$$\langle \mathcal{O}^R(^1D_2^{[1]})\rangle_{\rm NLO} = \left(1+\frac{\alpha_s\pi}{2v}C_F\right)\langle\mathcal{O}(^1D_2^{[1]})\rangle_{\rm LO}+\ldots, \tag{42}$$

where "…" denotes terms at higher order in v.

Finally, combining the matrix elements given above with the short-distance coefficients, accordingly, we get the forward scattering amplitudes for the ^1L_J states computed by the NRQCD effective theory, which are summarized below:

$$(2\,\mathrm{Im}\mathcal{A}(^1S_0^{[1]}))|_{\mathrm{pertNRQCD}} = \frac{2\,\mathrm{Im}f(^1S_0^{[1]})}{m_Q^2}\left(1 + C_F\frac{\alpha_s\pi}{2v}\right)\langle\mathcal{O}(^1S_0^{[1]})\rangle_{\mathrm{LO}}, \tag{43a}$$

$$(2\,\mathrm{Im}\mathcal{A}(^1S_0^{[8]}))|_{\mathrm{pertNRQCD}} = \frac{2\,\mathrm{Im}f(^1S_0^{[8]})}{m_Q^2}\left[1 + \left(C_F - \frac{1}{2}C_A\right)\frac{\alpha_s\pi}{2v}\right]\langle\mathcal{O}(^1S_0^{[8]})\rangle_{\mathrm{LO}}, \tag{43b}$$

$$\begin{aligned}(2\,\mathrm{Im}\mathcal{A}(^1P_1^{[8]}))|_{\mathrm{pertNRQCD}} = &\left\{\frac{2\,\mathrm{Im}f(^1P_1^{[8]})}{m_Q^4}\left[1 + \left(C_F - \frac{1}{2}C_A\right)\frac{\alpha_s\pi}{2v}\right] - \frac{1}{2N_c}\frac{4\alpha_s}{3\pi m_Q^4}\frac{2\,\mathrm{Im}f(^1S_0^{[1]})}{\epsilon}\left(\frac{4\pi\mu^2}{\mu_\Lambda^2}\right)^\epsilon\Gamma(1+\epsilon)\right.\\ &\left. - \frac{4\alpha_s B_F}{3\pi m_Q^4}\frac{2\,\mathrm{Im}f(^1S_0^{[8]})}{\epsilon}\left(\frac{4\pi\mu^2}{\mu_\Lambda^2}\right)^\epsilon\Gamma(1+\epsilon)\right\}\langle\mathcal{O}(^1P_1^{[8]})\rangle_{\mathrm{LO}},\end{aligned} \tag{43c}$$

$$(2\,\mathrm{Im}\mathcal{A}(^1D_2^{[1]}))|_{\mathrm{pertNRQCD}} = \left[\frac{2\,\mathrm{Im}f(^1D_2^{[1]})}{m_Q^6}\left(1 + C_F\frac{\alpha_s\pi}{2v}\right) - \frac{4\alpha_s C_F}{3\pi m_Q^6}\frac{2\,\mathrm{Im}f(^1P_1^{[8]})}{\epsilon}\left(\frac{4\pi\mu^2}{\mu_\Lambda^2}\right)^\epsilon\Gamma(1+\epsilon)\right]\langle\mathcal{O}(^1D_2^{[1]})\rangle_{\mathrm{LO}}. \tag{43d}$$

Setting expressions in (44) equal to those in (26), respectively, and expanding $\mathrm{Im}f_n$ in the power of α_s, we obtain the IR finite short-distance coefficients up to $\mathcal{O}(\alpha_s^3)$:

$$2\,\mathrm{Im}f(^1S_0^{[1]}) = \frac{8\pi\alpha_s^2}{3} + \frac{\alpha_s^3}{27}\left(4(477 - 16N_f) + 12(33 - 2N_f)\ln\left(\frac{\mu^2}{4m_Q^2}\right) - 93\pi^2\right), \tag{44a}$$

$$2\,\mathrm{Im}f(^1S_0^{[8]}) = \frac{5\pi\alpha_s^2}{6} + \frac{5\alpha_s^3}{432}\left(16(153 - 4N_f) + 12(33 - 2N_f)\ln\left(\frac{\mu^2}{4m_Q^2}\right) - 129\pi^2\right), \tag{44b}$$

$$2\,\mathrm{Im}f(^1P_1^{[8]}) = \frac{\pi\alpha_s^2}{2} + \frac{\alpha_s^3}{108}\left\{-3(6N_f - 61)\ln\left(\frac{\mu^2}{4m_Q^2}\right) + 2\left[-(24N_f + 63\ln(2) + 725) + 119\pi^2 + 114\ln\left(\frac{\mu}{\mu_\Lambda}\right)\right]\right\}, \tag{44c}$$

$$2\,\mathrm{Im}f(^1D_2^{[1]}) = \frac{16\pi\alpha_s^2}{45} + \frac{\alpha_s^3}{1620}\left[78720 - 512N_f - 7263\pi^2 - 4032\ln(2) + 2880\ln\left(\frac{\mu}{\mu_\Lambda}\right) - 192(N_f - 9)\ln\left(\frac{\mu^2}{4m_Q^2}\right)\right], \tag{44d}$$

where the short-distance coefficients of the P wave and D wave are μ_Λ dependent. Their μ_Λ dependence will be canceled by that of the corresponding renormalized operators, which could be obtained by finding the derivative of both sides of (39)–(41) of μ_Λ. For Born quantities, $\frac{d\langle\mathcal{O}(^1L_J^{[1,8]})\rangle_{\mathrm{LO}}}{d\mu_\Lambda} = 0$. Then we obtain the renormalization group equations at leading order in v and α_s:

$$\begin{aligned}\frac{d\langle\mathcal{O}^R(^1P_1^{[8]})\rangle_{\mathrm{NLO}}}{d\ln\mu_\Lambda} &= \frac{8\alpha_s C_F}{3\pi m_Q^2}\langle\mathcal{O}(^1D_2^{[1]})\rangle_{\mathrm{LO}}, \qquad \frac{d\langle\mathcal{O}^R(^1S_0^{[1]})\rangle_{\mathrm{NLO}}}{d\ln\mu_\Lambda} = \frac{1}{2N_c}\frac{8\alpha_s}{3\pi m_Q^2}\langle\mathcal{O}(^1P_1^{[8]})\rangle_{\mathrm{LO}},\\ \frac{d\langle\mathcal{O}^R(^1S_0^{[8]})\rangle_{\mathrm{NLO}}}{d\ln\mu_\Lambda} &= \frac{8\alpha_s B_F}{3\pi m_Q^2}\langle\mathcal{O}(^1P_1^{[8]})\rangle_{\mathrm{LO}}.\end{aligned} \tag{45}$$

The solutions of the matrix elements $\langle 1^1D_2|\mathcal{O}(\mu_\Lambda)|1^1D_2\rangle$ in the heavy quarkonium D-wave state $^1D_2$ are

$$\begin{aligned}\langle 1^1D_2|\mathcal{O}^R(^1P_1^{[8]})(\mu_\Lambda)|1^1D_2\rangle &= \frac{8C_F}{3m_Q^2 b_0}\ln\frac{\alpha_s(\mu_{\Lambda_0})}{\alpha_s(\mu_\Lambda)}\langle 1^1D_2|\mathcal{O}(^1D_2^{[1]})|1^1D_2\rangle,\\ \langle 1^1D_2|\mathcal{O}^R(^1S_0^{[1]})(\mu_\Lambda)|1^1D_2\rangle &= \frac{C_F}{4N_c}\left(\frac{8}{3m_Q^2 b_0}\ln\frac{\alpha_s(\mu_{\Lambda_0})}{\alpha_s(\mu_\Lambda)}\right)^2\langle 1^1D_2|\mathcal{O}(^1D_2^{[1]})|1^1D_2\rangle,\\ \langle 1^1D_2|\mathcal{O}^R(^1S_0^{[8]})(\mu_\Lambda)|1^1D_2\rangle &= \frac{C_F B_F}{2}\left(\frac{8}{3m_Q^2 b_0}\ln\frac{\alpha_s(\mu_{\Lambda_0})}{\alpha_s(\mu_\Lambda)}\right)^2\langle 1^1D_2|\mathcal{O}(^1D_2^{[1]})|1^1D_2\rangle,\end{aligned} \tag{46}$$

where the initial matrix elements like $\langle 1^1D_2|\mathcal{O}^R(^1P_1^{[8]})(\mu_{\Lambda_0})|1^1D_2\rangle$ at $\mu_{\Lambda_0} = m_Q v$ are eliminated [1,7,8].

To justify the elimination of initial matrix elements at $\mu_{\Lambda_0} = m_Q v$, we will compare our method with an alternative one in the potential NRQCD (pNRQCD) [35], where the soft scale $m_Q v$ in NRQCD is integrated out. Take spin-singlet S-wave color-octet matrix element $\langle h_Q|\mathcal{O}(^1S_0^{[8]})|h_Q\rangle$, for example. In NRQCD [1], it is determined by operator evolution equation

$$\langle h_Q|\mathcal{O}(^1S_0^{[8]})(\mu_\Lambda)|h_Q\rangle = \langle h_Q|\mathcal{O}(^1S_0^{[8]})(\mu_{\Lambda_0})|h_Q\rangle + \frac{4C_F}{3N_c b_0 m_Q^2}\ln\frac{\alpha_s(\mu_{\Lambda_0})}{\alpha_s(\mu_\Lambda)} \times \langle h_Q|\mathcal{O}(^1P_1^{[1]})|h_Q\rangle. \quad (47)$$

As proposed in [1], the second term on the right-hand side of Eq. (47) is enhanced by $\ln\frac{\alpha_s(\mu_{\Lambda_0})}{\alpha_s(\mu_\Lambda)}$ and the first term may be neglected, if the difference between the two scales μ_{Λ_0} and μ_Λ is large enough. However, in our case we have $\ln\frac{\alpha_s(m_c v)}{\alpha_s(2m_c)} = 1.10$ for charmonium and $\ln\frac{\alpha_s(m_b v)}{\alpha_s(2m_b)} = 0.738$ for bottomonium at $\mu_{\Lambda_0} = m_Q v$ and $\mu_\Lambda = 2m_Q$ (see the next section for the explicit input parameter values). Therefore, the $\ln\frac{\alpha_s(m_Q v)}{\alpha_s(2m_Q)}$ term does not contribute large enhancement; thus, the neglect of the first term in Eq. (47) should be carefully examined.

On the other hand, in pNRQCD [36,37], the color-octet matrix element can be related to the corresponding color-singlet one in the factorization form, for example [36],

$$\langle h_Q(nP)|\mathcal{O}(^1S_0^{[8]})|h_Q(nP)\rangle(\mu) = \frac{1}{9N_c^2 m_Q^2}\mathcal{E}(\mu)\langle h_Q(nP)|\mathcal{O}(^1P_1^{[1]})|h_Q(nP)\rangle, \quad (48)$$

where $h_Q(nP)$ denotes the n^1P_1 heavy quarkonium state, and at the leading-log approximation the nonperturbative constant $\mathcal{E}(\mu)$ is

$$\mathcal{E}(\mu) = \mathcal{E}(\mu') + \frac{24N_cC_F}{2b_0}\ln\frac{\alpha_s(\mu')}{\alpha_s(\mu)}. \quad (49)$$

Equation (49) is applicable to both charmonium and bottomonium. Substituting Eq. (49) into Eq. (48), one can get the leading-log behavior of the color-octet matrix element $\langle h_Q(nP)|\mathcal{O}(^1S_0^{[8]})|h_Q(nP)\rangle(\mu)$, which is consistent with that in NRQCD [1]. The authors of Ref. [36] fit the value of $\mathcal{E}(\mu)$ with the experimental data at $\mu = 1$ GeV and get

$$\mathcal{E}(\mu = 1\ \text{GeV}) = 5.3^{+3.5}_{-2.2}. \quad (50)$$

Setting $\mu' = m_Q v$ and using the central value given in Eq. (50), one can find a rough estimate:

$$\mathcal{E}(m_c v) = 2.01\frac{24N_cC_F}{2b_0}\ln\frac{\alpha_s(m_c v)}{\alpha_s(2m_c)} = 11.7, \quad (51)$$

which indicates that the initial matrix element could be neglected compared to the evolution term. While for bottomonium,

$$\mathcal{E}(m_b v) = 9.27\frac{24N_cC_F}{2b_0}\ln\frac{\alpha_s(m_b v)}{\alpha_s(2m_b)} = 8.51, \quad (52)$$

and the initial matrix element contributes at the same order as the evolution term. Considering theoretical uncertainties and experimental errors, our analysis above should be regarded as giving a reasonable qualitative estimate. Moreover, in Ref. [7], the same approximation was used to get the color-octet matrix elements for the ^3P_J charmonium states, and the obtained color-octet matrix elements are consistent with lattice QCD calculations and extracted values from the observed χ_{cJ} decays within 20–30% (see [7] for related references). Those conclusions are for the P-wave case, and we assume that they can be extended to D-wave case too. Our method of determining color-octet matrix elements in Eq. (46) may give the correct order of magnitude of the matrix elements, and is consistent with the pNRQCD approach proposed in [36,37].

V. NUMERICAL RESULTS AND PHENOMENOLOGICAL DISCUSSIONS

The long-distance matrix element of D-wave four-fermion color-singlet operator in the hadron state is related with the second derivative of radial wave function at the origin through the following relation:

$$\langle n^1D_2|\mathcal{O}(n^1D_2)|n^1D_2\rangle = \frac{15|R''_{nD}(0)|^2}{8\pi} = m_Q^6 H_{Dn}. \quad (53)$$

Combining the leading order coefficient $2\,\mathrm{Im}f(^1D_2^{[1]})_{\mathrm{LO}} = 16\pi\alpha_s^2/45$ given in (44d) and the color-singlet matrix element given in (53), one can reproduce the decay width of $^1D_2$ state in the CSM at leading order in α_s [10]:

$$\Gamma_{\mathrm{CSM}}(n^1D_2 \to gg) = \frac{2\alpha_s^2}{3}\frac{|R''_{nD}(0)|^2}{m_Q^6}. \quad (54)$$

However, there are contributions from the color-octet Fock states in (7) in NRQCD even at the order of α_s^2. The matrix elements of the P-wave octet operator and S-wave singlet as well as octet operators in the $^1D_2$ bound state could be estimated through the solutions of the operator evolution equations in (46).

The region of validity of the evolution equation is chosen as follows: the lower limit $\mu_{\Lambda_0} = m_Q v$ and the upper limit μ_Λ of order m_Q. For convenience, we take the factorization scale μ_Λ to be the same as the renormalization scale μ of order m_Q. We choose the pole mass $m_c = 1.5$ GeV, $v^2 = 0.3$, $\mu_{\Lambda_0} = m_c v$, $\mu_\Lambda = 2m_c$, $\alpha_s(2m_c) = 0.249$, $N_f = 3$, $\Lambda_{\mathrm{QCD}} = 390$ MeV, $H_{D1} = \frac{15|R''_{1D}(0)|^2}{8\pi m_c^6} = 0.786\times10^{-3}$ GeV [38] for charmonium, and $m_b = 4.6$ GeV, $v^2 = 0.1$, $\mu_{\Lambda_0} = m_b v$, $\mu_\Lambda = 2m_b$, $\alpha_s(2m_b) = 0.180$, $N_f = 4$, $\Lambda_{\mathrm{QCD}} = 340$ MeV, $H_{D1} = \frac{15|R''_{1D}(0)|^2}{8\pi m_b^6} = 0.401\times10^{-4}$ GeV for ^1D states and $H_{D2} = \frac{15|R''_{2D}(0)|^2}{8\pi m_b^6} = 0.750\times10^{-4}$ GeV for ^2D states [38] for bottomonium. The μ dependence curves of the decay widths are shown in Figs. 9 and 10. When $\mu = 2m_c$ for $c\bar{c}$ systems and $2m_b$ for $b\bar{b}$ systems, we get the predictions at $\mathcal{O}(\alpha_s^3)$

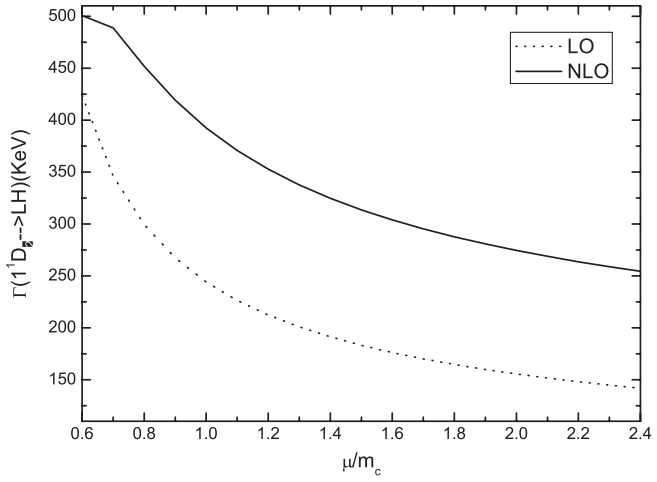

FIG. 9. Renormalization scale dependence of the decay width of charmonium state 1^1D_2 to light hadrons (LH).

$$\Gamma_C(1^1D_2 \to LH) = 274 \text{ KeV},$$
$$\Gamma_B(1^1D_2 \to LH) = 4.70 \text{ KeV}, \quad (55)$$
$$\Gamma_B(2^1D_2 \to LH) = 8.78 \text{ KeV}.$$

The LO decay widths for charmonium and bottomonium 1^1D_2 states are 155 KeV and 3.22 KeV. Therefore, the NLO QCD corrections contribute enhancement of factor 1.8 and 1.5, respectively.

For the 1^1D_2 charmonium state η_{c2}, the numerical values for all subprocesses are also listed in Table V. One can see from this table that the contributions from the Fock states other than $|^1D_2^{[1]}\rangle$ are dominant in the decay width, and the total result is about 1–3 times larger than that in CSM even at leading order in α_s.

For the phenomenological analysis of η_{c2}, we vary the renormalization/factorization scale from $2m_c$ to m_c and get

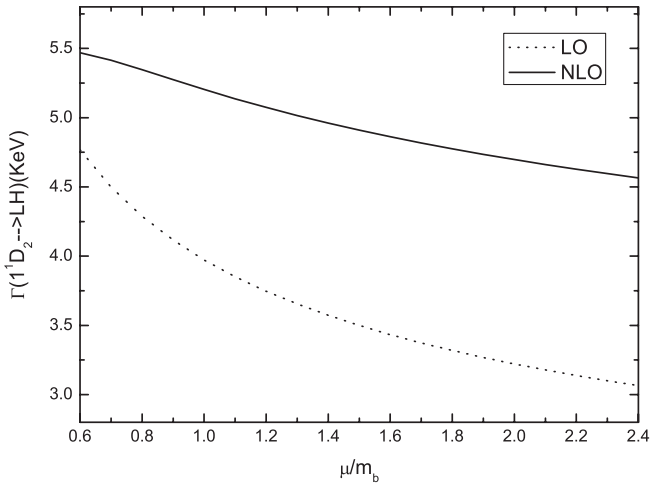

FIG. 10. Renormalization scale dependence of the decay width of bottomonium state 1^1D_2 to LH.

TABLE V. Subprocess decay rates of 1^1D_2 charmonium, where $m_c = 1.5$ GeV, $v^2 = 0.3$, $\mu_{\Lambda_0} = m_c v$, $\mu_\Lambda = 2m_c$, and $\alpha_s(2m_c) = 0.249$.

Subprocess	LO (KeV)	NLO (KeV)
$(^1D_2)_1 \to LH$	54.7	75.1
$(^1P_1)_8 \to LH$	66.6	132
$(^1S_0)_8 \to LH$	15.0	31.3
$(^1S_0)_1 \to LH$	19.2	36.1

$\Gamma(\eta_{c2} \to LH) = 274$–$392$ KeV. The electric transition rate $\Gamma(\eta_{c2} \to \gamma h_c) = 339$–$375$ KeV [13] and the dipion transition rate $\Gamma(\eta_{c2} \to \eta_c \pi\pi) \approx 45$ KeV [11] have been estimated elsewhere in the literature.

As emphasized before, the η_{c2} should be a narrow state, since its mass and quantum numbers forbid it to decay into charmed meson pairs $D\bar{D}$ and $D^*\bar{D}$. Therefore, the main decays modes of η_{c2} are expected to be the electric as well as hadronic transitions to lower-lying charmonium states and the inclusive light hadronic decay. With all these decay widths given above, we get the total width of η_{c2} to be about 660–810 KeV, and the branching ratio of the electric transition to be

$$\mathcal{B}(\eta_{c2} \to \gamma h_c) = (44\text{–}54)\%, \quad (56)$$

which provides important information on probing this missing state. In practice, one can search for η_{c2} through the cascade decay $\eta_{c2} \to \gamma h_c \to \gamma\gamma\eta_c \to \gamma\gamma K\bar{K}\pi$ with branching ratios $\mathcal{B}(h_c \to \gamma\eta_c) \approx 0.4$ [11,39] and $\mathcal{B}(\eta_c \to K\bar{K}\pi) \approx 7\%$ [40]. Similar decay chains can also be used to search for the $\eta_{b2}^{(\prime)}$.

The production rates of η_{c2} are expected to be generally low in many processes, because the rates are suppressed by the small values of the second derivative squared of the wave function at the origin, and also by its spin-singlet nature, which forbids η_{c2} to couple to a photon, or to be detected from the E1 transitions of higher spin-triplet charmonia. Nevertheless, efforts should be made to find this very unique missing charmonium state. Hopefully, the study for the inclusive light hadronic decay of η_{c2} in NRQCD will provide useful information on searching for this state in high-energy $p\bar{p}$ collision [14], in B decays [15], in higher charmonium transitions, in e^+e^- process in BESIII at BEPC [17], and particularly in the low-energy $p\bar{p}$ reaction in PANDA at FAIR [16].

VI. SUMMARY

In this paper, we calculate the inclusive light hadronic decay width of the $^1D_2$ heavy quarkonium state up to order of α_s^3 and at the leading order in v within the framework of NRQCD. We find that the inclusive decay widths into light hadrons via gluons and light quarks at order of α_s^3 in QCD suffer from both IR divergences and Coulomb singularities, but they can be absorbed into the renormalization of

the matrix elements of the four-fermion operators in NRQCD precisely. Therefore, after matching the full QCD onto NRQCD, the IR divergent part is removed, and IR finite short-distant coefficients are obtained, and the dependence on the factorization scale of the coefficient is canceled by that of the corresponding matrix element with the renormalization group analysis.

At leading order in α_s, the result in the CSM can be reproduced but there are many other contributions, such as that from color-octet P-wave operators, which will enhance the width in CSM by several times in magnitude even at the leading order in α_s. Furthermore, the NLO results give extra enhancement factors of 1.8 for η_{c2} and 1.5 for η_{b2} relative to the LO ones, respectively. By choosing the factorization scale as $2m_Q$, the light hadronic decay widths are found to be about 274, 4.7, and 8.8 KeV for the η_{c2}, η_{b2}, and η'_{b2}, respectively. Based on these estimates, and using the E1 transition width and dipion transition width for the η_{c2} estimated elsewhere in the literature, we get the total width of η_{c2} to be about 660–810 KeV, and the branching ratio of the electric transition $\eta_{c2} \to \gamma h_c$ to be about (44–54)%, which will be useful in searching for this missing charmonium state through, e.g., $\eta_{c2} \to \gamma h_c$ followed by $h_c \to \gamma \eta_c$.

ACKNOWLEDGMENTS

We would like to thank C. Meng and Y.-J. Zhang for useful discussions and reading the manuscript. Y. F. thanks R. Mertig and F. Maltoni for their useful suggestions by e-mail. Z. G. H. thanks the Institute of High Energy Physics of the Chinese Academy of Sciences and Theoretical Physics Center for Science Facilities for their hospitality. This work was supported in part by the National Natural Science Foundation of China, under Contract Nos. 10675003 and 10721063, and by the Ministry of Science and Technology of China under Contract No. 2009CB825200.

[1] G. T. Bodwin, E. Braaten, and G. P. Lepage, Phys. Rev. D **51**, 1125 (1995); **55**, 5853(E) (1997).
[2] See, e.g., J. H. Kühn, J. Kaplan, and E. G. O. Sadiani, Nucl. Phys. **B157**, 125 (1979); C. H. Chang, Nucl. Phys. **B172**, 425 (1980); W. Y. Keung, Phys. Rev. D **23**, 2072 (1981); J. H. Kühn and H. Schneider, Phys. Rev. D **24**, 2996 (1981); L. Clavelli, Phys. Rev. D **26**, 1610 (1982).
[3] G. T. Bodwin, E. Braaten, T. C. Yuan, and G. P. Lepage, Phys. Rev. D **46**, R3703 (1992).
[4] Han-Wen Huang and Kuang-Ta Chao, Phys. Rev. D **54**, 3065 (1996); **56**, 7472(E) (1997); **60**, 079901(E) (1999).
[5] Han-Wen Huang and Kuang-Ta Chao, Phys. Rev. D **55**, 244 (1997).
[6] Han-Wen Huang and Kuang-Ta Chao, Phys. Rev. D **54**, 6850 (1996); **56**, 1821(E) (1997).
[7] Zhi-Guo He, Ying Fan, and Kuang-Ta Chao, Phys. Rev. Lett. **101**, 112001 (2008).
[8] Zhi-Guo He, Ying Fan, and Kuang-Ta Chao (unpublished).
[9] G. Belanger and P. Moxhay, Phys. Lett. B **199**, 575 (1987); L. Bergstrom and P. Ernstrom, Phys. Lett. B **267**, 111 (1991).
[10] V. A. Novikov *et al.*, Phys. Rep. **41**, 1 (1978).
[11] Estia J. Eichten, Kenneth Lane, and Chris Quigg, Phys. Rev. Lett. **89**, 162002 (2002).
[12] E. J. Eichten, K. Lane, and C. Quigg, Phys. Rev. D **69**, 094019 (2004).
[13] T. Barnes, S. Godfrey, and E. S. Swanson, Phys. Rev. D **72**, 054026 (2005); B. Q. Li and K. T. Chao, Phys. Rev. D **79**, 094004 (2009).
[14] Frank Close, Phys. Lett. B **342**, 369 (1995); Peter L. Cho and Mark B. Wise, Phys. Rev. D **51**, 3352 (1995).
[15] Pyungwon Ko, Jungil Lee, and H. S. Song, Phys. Lett. B **395**, 107 (1997); F. Yuan, C. F. Qiao, and K. T. Chao, Phys. Rev. D **56**, 329 (1997).
[16] J. Ritman (PANDA Collaboration), arXiv:hep-ex/0702013.
[17] D. M. Asner *et al.*, arXiv:0809.1869.
[18] A. V. Manohar, Phys. Rev. D **56**, 230 (1997).
[19] M. Beneke and V. A. Smirnov, Nucl. Phys. **B522**, 321 (1998).
[20] F. Maltoni, PhD thesis, University of Pisa, 1999.
[21] E. Braaten and J. Lee, Phys. Rev. D **67**, 054007 (2003); **72**, 099901(E) (2005).
[22] A. Petrelli, M. Cacciari, M. Greco, F. Maltoni, and M. L. Mangano, Nucl. Phys. **B514**, 245 (1998).
[23] J. Novotny, Czech. J. Phys. **44**, 633 (1994).
[24] R. Mertig and W. L. van Neerven, Z. Phys. C **70**, 637 (1996).
[25] D. Kreimer, arXiv:hep-ph/9401354.
[26] S. A. Larin, Phys. Lett. B **303**, 113 (1993).
[27] P. Breitenlohner and D. Maison, Commun. Math. Phys. **52**, 11 (1977); **52**, 39 (1977); **52**, 55 (1977).
[28] G. T. Bodwin and A. Petrelli, Phys. Rev. D **66**, 094011 (2002).
[29] R. Ticciati, *Quantum Field Theory For Mathematicians* (Cambridge University Press, United Kingdom, 1999).
[30] Wai-Yee Keung and I. J. Muzinich, Phys. Rev. D **27**, 1518 (1983).
[31] J. Küblbeck, M. Böhm, and A. Denner, Comput. Phys. Commun. **60**, 165 (1990); T. Hahn, Comput. Phys. Commun. **140**, 418 (2001).
[32] R. Mertig, M. Böhm, and A. Denner, Comput. Phys. Commun. **64**, 345 (1991).
[33] M. Klasen, B. A. Kniehl, L. N. Mihaila, and M. Steinhauser, Nucl. Phys. **B713**, 487 (2005).
[34] H. W. Griesshammer, arXiv:hep-ph/9804251.
[35] N. Brambilla, A. Pineda, J. Soto, and A. Vairo, Rev. Mod.

Phys. **77**, 1423 (2005).
[36] N. Brambilla, D. Eiras, A. Pineda, J. Soto, and A. Vairo, Phys. Rev. Lett. **88**, 012003 (2001).
[37] N. Brambilla, D. Eiras, A. Pineda, J. Soto, and A. Vairo, Phys. Rev. D **67**, 034018 (2003).
[38] E. J. Eichten and C. Quigg, Phys. Rev. D **52**, 1726 (1995).
[39] K. T. Chao, Y. B. Ding, and D. H. Qin, Phys. Lett. B **301**, 282 (1993).
[40] C. Amsler *et al.* (Particle Data Group), Phys. Lett. B **667**, 1 (2008).